Effects of in vivo Flip Angle Variations on the Accuracy of DCE-MRI Perfusion Parameters at 1.5T and 3.0T

Jiangsheng Yu[1], Xia Zhao[1], Yiqun Xue[1], Mark A Rosen[1], Christina S Chu[2], and Hee Kwon Song[1]

[1]*Departments of Radiology, University of Pennsylvania, Philadelphia, PA, United States,* [2]*Obstetrics and Gynecology, University of Pennsylvania, Philadelphia, PA, United States*

Introduction: Dynamic contrast-enhanced (DCE)-MRI of tumors has emerged as one of the prime methods for assessing the effectiveness of antiangiogenic and antivascular agents. In DCE-MRI, a dynamic series of T1-weighted images is acquired during intravenous bolus injection of a contrast agent and the measured signal subsequently fitted to a model to quantify perfusion parameters, such as K^{trans} and v_e. During the fitting procedure, most current studies assume that the prescribed nominal flip angles are accurately played out. It was previously shown that large flip angle variations can exist throughout the FOV which can cause substantial errors in perfusion measurements in coronal sections of the body on a standard 1.5T MRI system [1]. In this work, we compare the flip angle variations and its effects on the accuracy of K^{trans} and v_e for different orientation planes on three different scanners: standard 1.5T and 3.0T systems (Siemens Sonata and Trio), as well as on a short-bore 1.5T system (Siemens Espree) to determine whether higher fields and short bore systems potentially exacerbates these measurement inaccuracies.

Methods: Actual flip angle imaging (AFI) [2] was applied to determine the in vivo flip angle variability. A 3D golden-angle hybrid radial acquisition scheme was modified for AFI from a conventional spoiled gradient-echo sequence [3]. To obtain T1-weighted AFI images, combined random RF phase and random gradient moment were applied to take advantage of radial acquisition for complete spoiling of transverse magnetizations [4]. The AFI sequence parameters were as follows: TR_1/TR_2=6/24ms, TE=1.7ms, FOV=400mm, slice thickness=8mm, 32 slices, angular views=600 (scan time=9.6min), readout points=384 (including 2x oversampling), bandwidth=530Hz/pixel, 6 channels. The nominal AFI flip angles for the standard 3.0T, 1.5T and the short bore 1.5T were 34, 48 and 60 degrees, respectively, and were varied due to SAR limitations. Flip angle deviations were computed pixel-wise, and based on these measurements the potential errors in K^{trans} and v_e throughout the body were computed based on simulations. In the simulation the following parameter values were used to generate a DCE-MRI dataset: K^{trans}=0.4 min^{-1}, v_e=0.4, and v_p=0.02. The flip angle used to generate the DCE-MRI signal (25°) was adjusted to reflect the fractional deviations observed in the flip angle maps. For the arterial input function, an experimentally-derived functional form based on a population-averaged input function described previously was utilized [6]. Subsequently, DCE-MRI data were fit to the Tofts' model using the assumed nominal flip angle (25°) to compute the perfusion parameters. The simulation assumed the correct value of intrinsic tumor and blood T_1 (e.g. acquired with an IR sequence) and the same flip angle for the AIF and tissue (which assumes the ideal condition in which the two are in close proximity).

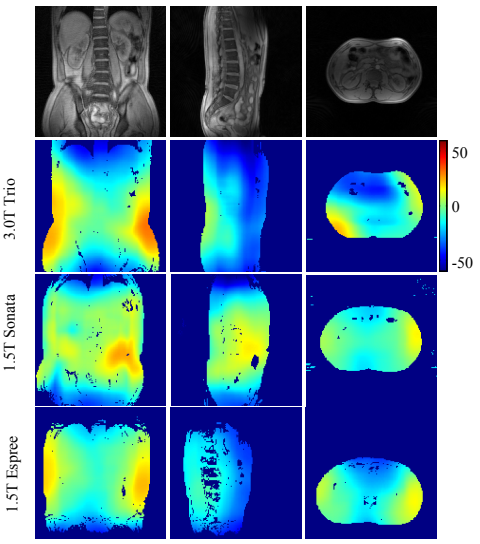

Fig. 1 Anatomic images (coronal, sagittal and axial, from left to right), and the corresponding flip angle error maps (% error).

Results and Discussion: Figure 1 shows the flip angle error maps at the central slices of the three orientations on the three systems. Large flip angle variations occur throughout the body in all three orientations along both superior/inferior and lateral regions of the torso. Figure 2 shows the resulting K^{trans} errors, and Table 1 compares the flip angle deviations and errors in perfusion values. Table 1 indicates that standard deviations of the flip angles are similar for the three MRI systems, which suggests that over a large region of the body the B1 field homogeneity is not significantly exacerbated at higher fields and short bore systems. Table 1 also shows the average flip angle deviation is smallest for the standard 1.5T scanner. However, it should be noted that the average flip angle is dependent on the RF amplifier gain which is determined by the scanner's calibration procedure and can differ from one scan to next. On the other hand, the standard deviation of the flip angles, determined both by the extent of the MR hardware and finite wavelength effects within the object, is expected to remain more stable. This was confirmed in a repeat study on the Espree system: while the mean flip angle deviation increased by 6.7% (e.g. from -23.4 to -31.7% for sagittal), the standard deviations remained nearly identical. Unlike K^{trans}, accuracy of v_e is not substantially affected by these flip angle deviations.

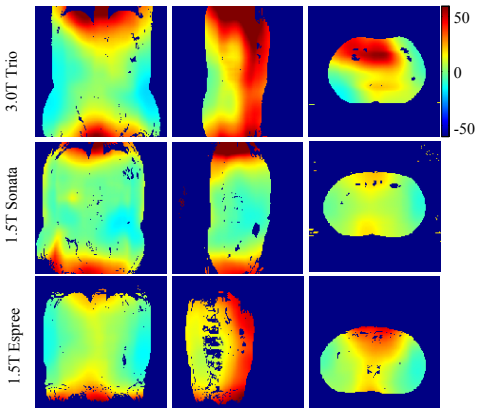

Fig. 2 Corresponding errors in K^{trans} at different locations throughout the body. Errors are in %.

Conclusion: The current work shows that there are similar degrees of flip angle variations throughout the body on both 1.5T and 3T systems which can cause substantial errors in perfusion measurements along all orientations. These errors can potentially mask true changes in tumor treatment response, and flip angle mapping may be a crucial part of every DCE-MRI protocol, in particular when lesions are located peripherally in large FOV protocols.

Table 1 Comparison of flip angle, K^{trans} and v_e errors (in %) for the middle 20 slices of the three orientations. Shown are the mean ± standard deviation.

	3.0T Trio			1.5T Sonata			1.5T Espree (short-bore)		
	Coronal	Sagittal	Axial	Coronal	Sagittal	Axial	Coronal	Sagittal	Axial
Flip angle	-20.7±21.0	-28.8±13.6	-21.0±17.0	-5.4±17.9	-10.5±16.1	-7.7±16.6	-13.9±16.4	-23.4±9.4	-13.4±15.0
K^{trans}	26.6±27.8	34.8±20.6	25.2±22.5	7.8±18.9	12.5±19.4	14.8±20.2	16.2±19.5	25.8±12.7	15.1±16.8
v_e	0.03±0.67	0.27±0.51	0.23±0.52	-0.06±0.63	0.14±0.48	-0.50±0.76	0.21±0.50	0.52±0.21	0.27±0.46

Acknowledgments: American Cancer Society RSG-08-118-01-CCE; NIH P41-RR02305; NIH R01-CA125226; NIH UL1RR024134; NIH CA016520.

References: (1) Yu et al. ISMRM 2011:1076. (2) Yarnykh et al. Magn Reson Med 2007; 57:192-200. (3) Lin et al. Magn Reson Med 2008; 60: 1135–1146. (4) Lin et al. Magn Reson Med 2009; 62: 1185–1194. (5) Parker et al. Magn Reson Med 2006; 56: 993.